CHEMISTRY OF MATERIALS

ARTICLE

pubs.acs.org/cm

Click Chemistry on Solution-Dispersed Graphene and Monolayer CVD Graphene

Zhong Jin, Thomas P. McNicholas, Chih-Jen Shih, Qing Hua Wang, Geraldine L. C. Paulus, Andrew J. Hilmer, Steven Shimizu, and Michael S. Strano*

Department of Chemical Engineering, Massachusetts Institute of Technology, Cambridge, Massachusetts 02139, United States

ABSTRACT: Graphene from two different preparative routes was successfully functionalized with 4-propargyloxybenzenediazonium tetrafluoroborate in order to study a subsequent attachment by click chemistry (1,3-dipolar azide−alkyne cycloaddition) of a short chain polyethylene glycol with terminal carboxylic end group (PEG-COOH). The reaction steps were studied by FTIR and Raman spectroscopies, as well as zeta-potential and surface tension measurements. In the first route, pristine graphene was surfactant dispersed from a stage controlled expanded graphite before reaction, resulting in colloidally stable dispersions after dialysis removal of the surfactant following the two functionalization steps. The chemistry was shown to increase the zeta-potential from −45.3 to −54.6 mV and increase the surface tension from 48.5 to 63.0 mN/m compared to those of the precursor solution. The magnitudes of the zeta-potential and the resulting solution concentration were shown to increase with grafting density up to 14.2 μg/mL. A colloidal stability model was used to estimate the maximum grafting density of the PEG-COOH groups yielding a value of 1 per 10 nm^2. Raman mapping before and after the two-step functionalization suggests that edges and defects are preferentially reacted. In the second route, we investigated the same click chemistry functionalization on chemical vapor deposition (CVD) synthesized monolayer graphene films, which showed higher reactivity than solution-dispersed graphene. Because these methods do not originate with the more oxidized forms of graphene, the results point to new ways of more precisely controlling the chemistry of graphene.

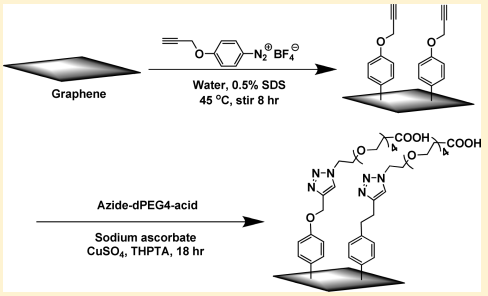

KEYWORDS: graphene, click chemistry, surface functionalization

INTRODUCTION

Graphene has attracted significant research interest due to its remarkable electrical, thermal, and mechanical properties that arise from the structure of its two-dimensional hexagonal carbon lattice.[1] There is an interest in covalently tethering polymeric, protein, or nanoparticle functionalities to graphene toward the development of novel composites,[2] biosensors,[3] and catalysts.[4] Covalent attachment to the graphene lattice directly is preferred for certain applications such as interfacial bonding of graphene in composites[5] or surface coatings, irreversible binding and display of certain biological molecules, and as stable receptors for sensor technologies.[6] Additionally, there has been a resurgence of interest in graphene oxide as a more easily solution-processable form of graphene.[7−11] However, these oxides necessarily result in disordered lattices containing some combination of carboxyl, epoxide, hydroxyl, and carbonyl groups.[8,12−14] As advances in the solution phase chemistry of graphene are made,[15,16] graphene with more precise and uniform functionality can replace these solutions for more precise engineering of the graphene interface in applications such as polymer matrices.[17−19]

The modification of graphene with diazonium functionalization is emerging as a versatile method for tailoring the chemical and electronic properties of graphene. Aryl diazonium salts have been demonstrated by several groups to attach covalently to mechanically exfoliated graphene layers,[20−24] epitaxial graphene grown on SiC substrates,[25,26] chemically converted graphene,[27,28] and solution-processable graphene.[29] The covalent attachment of diazonium groups on graphene has been shown to dope the graphene[20,21,30] and open a band gap.[31] In addition to these electronic changes, chemical changes can be imparted to the graphene by tailoring the functional groups on the diazonium moiety by organic synthetic chemistry. This chemical handle also allows subsequent reactions to attach additional moieties,[32] which will have an important role in incorporating graphene into composite materials and chemical and biological sensors.

The reactivity of graphene differs from that of carbon nanotubes in several important ways. The curvature in the latter offers an additional selectivity, as the strain energy per carbon[33] increases with decreasing diameter. Hence, the graphene lattice itself is expected to be less reactive than nanotube counterparts for ring-opening or oxidative reactions.[34] The zigzag edge of graphene nanoribbons has been theoretically predicted to be particularly reactive.[35] Previous work by our group and subsequently by others have shown that the diazonium electron transfer reaction occurs more readily at the edges of graphene sheets rather than in the bulk of the basal plane[23,24,36] and that the reactivity of a single layer of graphene is higher than that of two or more layers.[22,24]

Received: April 20, 2011
Revised: June 9, 2011
Published: June 30, 2011

Scheme 1. Diazonium Reaction and Subsequent Click Chemistry Functionalization on Graphene Sheets

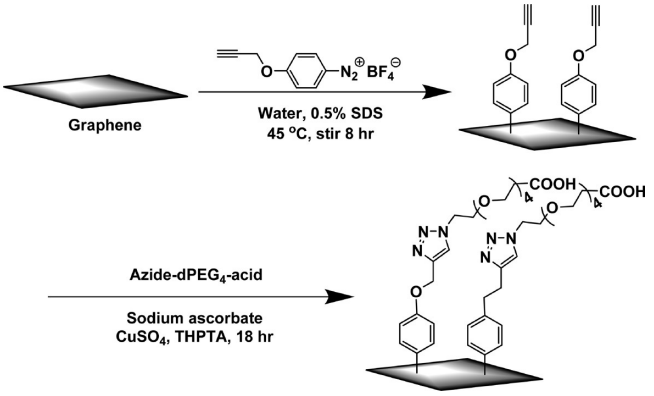

The copper-catalyzed Huisgen 1,3-dipolar azide−alkyne cycloaddition reaction has been used extensively to achieve selective covalent coupling between chemical moieties at mild conditions,[37,38] particularly for organic synthesis,[39] surface modification,[40] and bioconjugation.[41,42] This reaction has also been applied to nanoparticles[43,44] and recently to the chemical modification of carbon nanotubes.[45] However, its use for the chemistry of graphene and its derivatives remains limited. Recently, the immobilization of alkyl groups[46] and polystyrene[47] onto graphite or graphene oxide by click chemistry was reported. However, the functionalization via click chemistry of nonoxidized graphene (pristine graphene) remains to be fully investigated. This approach should be generic and lead to synthetic approaches that may displace harsher oxidative treatments that yield a wide spectrum of chemical functionalities on the graphene surface, as in the case of Hummer's method and graphite oxide.

In this article, we explore the 1,3-dipolar azide−alkyne cycloaddition reaction on previously unfunctionalized (pristine) graphene sheets prepared by several means. In the first, we use expanded graphite prepared from a method recently developed in our laboratory,[48] which yields a solution of graphene flakes dispersed in sodium cholate and water. In the second, we use monolayer graphene produced from CVD grown in our laboratory.[49] The general approach to click chemistry follows Scheme 1. Here, the alkyne groups are introduced onto graphene sheets by reaction with 4-propargyloxybenzenediazonium tetrafluoroborate. Subsequently, short polyethylene glycol chains are grafted onto the graphene lattice via the azide−alkyne cycloaddition reaction. Using this method, it is possible to create water-soluble graphene suspended without surfactants and without oxidative treatment.

EXPERIMENTAL SECTION

Preparation of Aqueous Dispersed Graphene. Aqueous-phase dispersions of unfunctionalized, few-layer exfoliated graphene (solution-phase graphene or SP-graphene) with 2 wt % sodium cholate surfactant were prepared as described by our laboratory previously.[48] Briefly, Stage-2 iodine chloride intercalated highly ordered pyrolytic graphite (HOPG) was thermally expanded at 800 °C and then dispersed in 2 wt % sodium cholate aqueous solution by slow homogenization and low-power ultrasonication, resulting in a supernatant solution of graphene flakes. After dispersion, the SP-graphene flakes were deposited on SiO_2/Si substrates and size sorted using the Marangoni "coffee ring" effect[50] as we have also described previously.[48] Briefly, consider the drying process of a droplet of graphene dispersion on the hydrophilic SiO_2 substrate with a prescribed contact angle. Because the evaporation rate is greatest at the edge, there is an internal flow of fluid that moves particulate matter within the droplet either toward or away from the edge (depending on whether the contact area or contact angle is pinned). This flow can sort graphene flakes by size, as we have shown previously. Graphene flakes deposit along the edge of the drop under the conditions used in this work. The presence of these flakes facilitates the pinning of the contact line at the drop edge. During the evaporation process, since the evaporation rate is greatest at the edge, an outward Marangoni flow of liquid is induced from the bulk of the drop, and the contact angle becomes smaller gradually. The liquid flow carries out graphene flakes toward the edge of the drop which results in the formation of the "coffee ring". In the flow field, large graphene flakes have a higher probability to contact the substrate and subsequently deposit onto the surface. As a result, the graphene flakes are separated on the basis of lateral size but independently of their thickness. Typically, a 10 μL drop of pristine SP-graphene suspension was dropped on a SiO_2/Si chip with 300 nm thermally oxidized silica and dried in the atmosphere to form SP-graphene flake "coffee rings" induced by the Marangoni effect. Then the SiO_2/Si chip was washed generously with Milli-Q water to remove the surfactant and dried with a nitrogen gun.

Preparation of Monolayer CVD Graphene. Large-area single-layer graphene films grown by the CVD method (CVD-graphene) on copper foils were transferred to the surface of oxygen plasma cleaned SiO_2/Si chips (with 300-nm-thick thermally grown SiO_2 layer) or quartz glass slides.[49,51] Typically, a ~4 cm^2 copper foil (Aldrich, 99.999%, 25 μm thick) was placed at the center of a 1-inch-diameter fused quartz tube in a tube furnace. The furnace tube was evacuated and heated to 1000 °C under a 400 sccm H_2 gas flow with a pressure of ~1.5 KPa. After annealing for 30 min under these conditions, a CH_4 gas flow of 20 sccm was introduced, and the temperature in the furnace tube was maintained for 6−8 min. The CH_4 gas flow was stopped after the growth period. The copper foil was cooled to room temperature under H_2 gas flow and taken out from the tube furnace. A poly(methyl methacrylate) (PMMA) film was spin-coated (3,000 rpm, 1 min) onto the copper foil covered with CVD-graphene film and heated up to 60 °C for 5 min to cure the PMMA film. Then the PMMA/CVD-graphene layer was separated from the copper foil by etching in a 1 M $CuCl_2$/6 M HCl aqueous solution and then placed on the surface of Milli-Q water to remove any water-soluble residues. The PMMA/CVD-graphene film was then transferred to the designated substrate and dried with a nitrogen gun. The PMMA film was dissolved away by soaking the substrate in acetone for 10 h, thus leaving only the CVD-graphene sheets remaining on the substrates. The CVD-graphene samples were annealed at 350 °C in an argon atmosphere under vacuum for 2 h in order to remove any possible contamination.

Reagent Preparation. 4-Propargyloxybenzenediazonium tetrafluoroborate was prepared in three steps. First, 4-nitrophenyl propargyl ether was prepared by etherification of 4-nitrophenol with propargyl bromide;[45] second, 4-nitrophenylpropargyl ether was reduced to 4-aminophenylpropargyl ether;[52] third, 4-propargyloxybenzenediazonium tetrafluoroborate was obtained by the diazotization of 4-aminophenyl-propargyl ether and recrystallized with ether.[33] The identity of the final product was confirmed by nuclear magnetic resonance (NMR): ^{1}H NMR (400 MHz, $CDCl_3$), ppm δ = 3.05 (s, ≡C−H, 1H), 5.04 (d, CH_2, 2H), 7.42 (d, Ar−H, 2H) and 8.46 (d, Ar−H, 2H). The short-chain polyethylene glycol with azido and carboxyl end-groups (azido-dPEG$_4$-acid) was purchased from Quanta BioDesign Ltd., USA. Other chemicals were obtained from Sigma-Aldrich.

Diazonium Functionalization of Graphene. Typically, 25 mg of sodium dodecylsulfate (SDS) was dissolved into 5 mL of SP-graphene aqueous dispersion, and then 5 mg of 4-Propargyloxybenzenediazonium

Table 1. Comparison of Surface Tension and Zeta-Potential of the Pristine and PEG-COOH Functionalized SP-Graphene Aqueous Suspensions

samples	optical absorbance at 660 nm	concentration (μg/mL)	surface tension (mN/m)	zeta-potential (mV)
unfunctionalized SP-graphene in Milli-Q water with 2 wt % sodium cholate	0.283	41.0	48.5	−45.3
functionalized SP-graphene in Milli-Q water after dialysis	0.098	14.2	63.0	−54.6
unfunctionalized SP-graphene in Milli-Q water after dialysis	0.010	1.5	55.4	−21.7

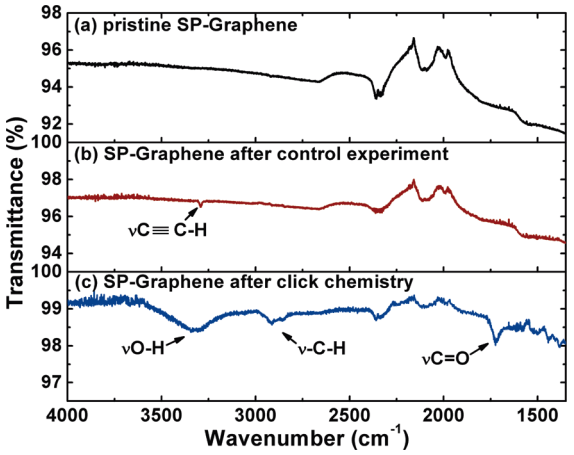

Figure 1. ATR-IR spectra of (a) pristine SP-graphene, (b) SP-graphene after the control experiment where no $CuSO_4$ was added in the click chemistry reaction, and (c) SP-graphene after undergoing the diazonium reaction and subsequent click chemistry reaction. All of the spectra were collected on the SP-graphene flakes loaded on Teflon films with 0.22 μm micropores.

tetrafluoroborate was added into the mixture. The mixture was heated to 45 °C and stirred vigorously for 8 h. After the reaction, the resulting suspension was filtered on a Teflon membrane (0.22 μm pore size) and subsequently washed by 100 mL of Milli-Q water and acetone. Then the alkynyl-functionalized SP-graphene flakes were redispersed in 5 mL of 1 wt % SDS/water solution by low-power ultrasonication (40 kHz, 10 min) for the following click chemistry process. For a second set of experiments performed on substrates, the substrates loaded with drop-dried SP-graphene flake "coffee rings" or transferred CVD-graphene films were immersed in 5 mL of Milli-Q water to replace the SP-graphene aqueous dispersion in this reaction and the following click chemistry reaction. After the reactions, the substrates were washed generously with Milli-Q water and acetone to remove residues.

Copper-Catalyzed 1,3-Dipolar Azide−Alkyne Cycloaddition on Graphene. Seven milligrams of sodium bicarbonate and ~13 μL of azido-dPEG$_4$-acid solution (0.19 M in Milli-Q water, 2.5 μmol) were dissolved into 5 mL of the alkynyl-functionalized SP-graphene suspension. Then, 1.2 mL of a premixed aqueous solution of 0.5 mM $CuSO_4$ and 2.5 mM tris(3-hydroxypropyltriazolylmethyl)amine (THPTA) was added into the suspension. After sufficiently mixing, 6 mg of sodium ascorbate was dissolved into the suspension as the reductant. The mixture was stirred vigorously for 18 h. The suspension was filtered on a Teflon membrane (0.22 μm pore size) and washed with 100 mL of Milli-Q water, and then redispersed in 5 mL of 1 wt % SDS/water solution by mild ultrasonication (40 kHz, 10 min). In control experiments, this click chemistry process was also performed under the same conditions but without adding any copper catalyst.

Characterization of Reacted Graphene. Attenuated total reflection infrared spectroscopy (ATR-IR) was used to detect the characteristic absorbance of functional groups grafted on SP-graphene flakes and monolayer CVD-graphene sheets. The aqueous dispersbility of pristine and PEG-COOH functionalized SP-graphene was monitored by UV−vis absorption spectroscopy after dialysis against Milli-Q water. Briefly, 3 mL of pristine or PEG-COOH functionalized SP-graphene suspension in a dialysis bag (with a MWCO of 10,000 g/mol) was dialyzed against 2 L of Milli-Q water for 4 days with 8 changes of water to remove the remaining surfactant. Surface tension and zeta-potential analysis were also taken to investigate the colloidal stability of the pristine and functionalized SP-graphene flakes (Table 1). To determine the degree of functionalization, atomic force microscopy (AFM) and Raman spectroscopy signals were, respectively, collected on SP-graphene flakes before and after the grafting of organic species; as a control, Raman mappings on the as-prepared and PEG-COOH functionalized CVD-graphene films was also conducted.

RESULTS AND DISCUSSION

The 4-propargyloxyphenyl groups grafted on graphene sheets by the diazonium reaction can be used for the binding of additional species through click chemistry (Scheme 1). In this work, azido-dPEG$_4$-acid was chosen for the click chemistry for two reasons: the short-chain polyethylene glycol and carboxyl groups can be easily distinguished by ATR-IR, and also, such groups can promote the colloidal dispersion of graphene in water upon dialysis removal of the surfactant, creating an alternative to the widely used graphene and graphite oxide. Hence, there is a clear and direct physical test of whether a useful grafting density can be achieved if the resulting graphene can be suspended directly in water without surfactant. We utilize THPTA, an accelerating ligand with affinity for Cu, with $CuSO_4$ as the click chemistry catalyst.[42] As shown in Figure 1, the ATR-IR characteristic absorbance of the relevant functional groups grafted to SP-graphene was detected. The ATR-IR spectrum (Figure 1c) of SP-graphene after the click chemistry reaction shows a band at ~1730 cm^{-1} associated with the C═O stretching vibrations of carboxyl groups as well as a wide band at ~3330 cm^{-1}, which may be attributable to O−H stretching vibrations of carboxyl groups. The peaks at ~2880 cm^{-1} are consistent with the symmetric stretching of alkyl C−H bonds in the polyethylene glycol chains, compared with the ATR-IR spectrum of the azido-PEG-COOH reagent and the IR data in the literature.[53] These absorption peaks indicate that the polyethylene glycol chains with carboxyl end-groups were successfully grafted on the SP-graphene flakes. As a control, the click reaction was also carried out on 4-propargyloxyphenyl functionalized SP-graphene without adding $CuSO_4$. As shown in Figure 1b, The ATR-IR spectrum of the control sample shows the remaining ≡C−H stretch at ~3300 cm^{-1}, from the unreacted 4-propargyloxyphenyl groups. Also, no features of polyethylene glycol or carboxyl groups can be observed.

dx.doi.org/10.1021/cm201131v |Chem. Mater. 2011, 23, 3362–3370

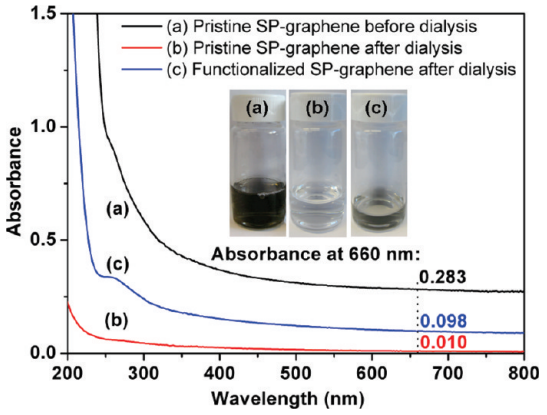

Figure 2. UV−vis absorbance spectra and optical images of (a) pristine SP-graphene aqueous suspension stabilized by 2 wt % sodium cholate surfactant, (b) pristine SP-graphene supernatant in water after dialysis against Milli-Q water, and (c) PEG-COOH functionalized SP-graphene supernatant in water after dialysis against Milli-Q water.

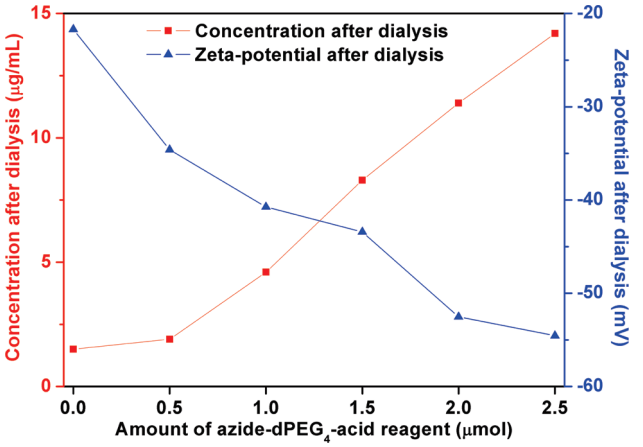

Figure 3. The plot of the concentration and zeta-potential of PEG-COOH functionalized SP-graphene aqueous suspensions after dialysis against Milli-Q water versus the amount of azide-dPEG$_4$-acid reagent added to the click chemistry reactions.

The resulting aqueous dispersions before and after the two-step functionalization were characterized by UV−vis spectroscopy after dialysis against Milli-Q water for 4 days with 8 changes of water to remove the surfactant, as shown in Figure 2. The measured optical absorbance of the original SP-graphene aqueous suspension stabilized by 2 wt % sodium cholate surfactant is 0.283 (with absorption cell length of 1 cm) at a wavelength of 660 nm, corresponding to the SP-graphene concentration of ∼41.0 μg/mL.[48] After dialysis against Milli-Q water for 4 days, the sodium cholate surfactant was almost completely removed, and the precipitation of SP-graphene was found at the bottom of dialysis bag. The unfunctionalized SP-graphene supernatant in the dialysis bag was collected and measured by UV−vis spectroscopy, which shows an optical absorbance of 0.010, corresponding to a SP-graphene concentration of ∼1.5 μg/mL. Similarly, the optical absorbance of PEG-COOH functionalized SP-graphene supernatant in water was measured to be 0.098, indicating a concentration of ∼14.2 μg/mL. The UV−vis data showed that the saturated concentration of PEG-COOH functionalized SP-graphene in Milli-Q water was much higher than that of unfunctionalized SP-graphene, due to the grafted polyethylene glycol short-chain and carboxyl groups.

The surface tension and zeta-potential of pristine and PEG-COOH functionalized SP-graphene suspensions were also measured, as shown in Table 1. The surface tension of pristine SP-graphene aqueous suspension with 2 wt % sodium cholate surfactant is 48.5 mN/m, compared to the 72.1 mN/m surface tension for Milli-Q water at room temperature. The surface tension of pristine and PEG-COOH functionalized SP-graphene supernatants after dialysis against Milli-Q water is 55.4 and 63.0 mN/m, respectively. After dialysis, the PEG-COOH functionalized SP-graphene sample has a higher concentration but is less surface active than the pristine SP-graphene sample, which indicates that compared to the unfunctionalized material, the PEG-COOH functionalized SP-graphene flakes are more hydrophilic and prefer to remain solvated in the bulk water phase rather than at the water−air interface, as expected. The zeta-potential of the pristine SP-graphene aqueous suspension with 2 wt % sodium cholate is −45.3 mV, which shows the good stability of this colloid system. The zeta-potential of saturated pristine and PEG-COOH functionalized SP-graphene supernatants after dialysis is −21.7 mV and −54.6 mV, respectively, which indicates that the colloidal stability of PEG-COOH functionalized SP-graphene is much higher than pristine SP-graphene in aqueous dispersions. The results of the surface tension and zeta-potential analysis are consistent and indicate that the click chemistry approach to colloidal stability appears effective. To further investigate the influence of grafting densities on the stability of PEG-COOH functionalized graphene in aqueous dispersions, we also ran a series of control experiments with the different amounts of azid-dPEG$_4$-acid added to the click chemistry reactions, and all other conditions remained the same. As shown in Figure 3, along with the decrease in the amount of added azid-dPEG$_4$-acid reagent from 2.5 μmol to 0.5 μmol, the concentration of PEG-COOH functionalized SP-graphene aqueous dispersions after dialysis was decreased from 14.2 μg/mL to 1.9 μg/mL, and the zeta-potential was changed from −54.6 mV to −34.6 mV, indicating that a relatively high degree of grafting density is an important factor to stabilize the PEG-COOH functionalized SP-graphene in water.

To determine the degree of functionalization at different sites on the SP-graphene flakes, a second set of click chemistry experiments were performed on surface deposited SP-graphene flakes on SiO_2/Si substrates via a drop-dry process that size sorts the flakes as we have reported previously.[48] The experimental conditions of this on-chip graphene functionalization were the same as those for the aqueous suspensions. As shown in Figure 4a, a single SP-graphene flake near a SP-graphene "coffee ring" was observed via an optical microscope. Typical Raman spectra collected at the same position on this few-layer SP-graphene flake are shown in Figure 4b. The 2D band structure has a broad (∼60 cm^{-1}) full-width-at-half-maximum and shows a sum of four Lorentzian peaks; the shape of 2D band is comparable to the obtained 2D Raman spectra of bilayer Scotch-tape graphene on the same substrates with 633 nm in the literature[48,54,55] owing to the contributions of four different possible excitations.[56] After the functionalization, the G peak position of SP-graphene up-shifted from 1578 cm^{-1} to 1582 cm^{-1}, the intensity of D peak increased, and an accompanied D' peak at 1620 cm^{-1} appeared, which indicates the occurrence of graphene functionalization. The D/G band intensity ratio (I_D/I_G) reveals the in-plane crystallite dimension

dx.doi.org/10.1021/cm201131v |*Chem. Mater.* 2011, 23, 3362–3370

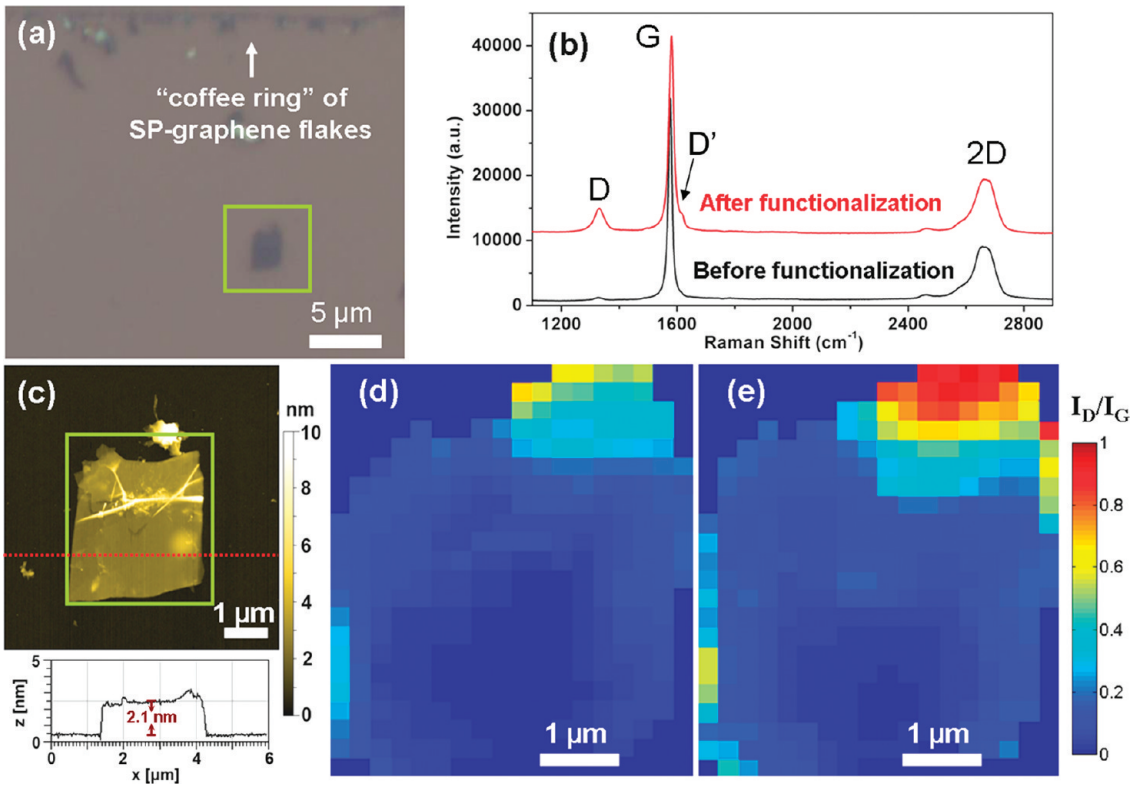

Figure 4. (a) Optical image of a SP-graphene flake near a drop-dried SP-graphene "coffee ring" on the surface of a SiO_2/Si chip with 300 nm thermally oxidized silica. (b) Typical Raman spectra taken at the same position of this few-layer SP-graphene flake before and after undergoing the two-step functionalization. (c) AFM image of this SP-graphene flake. A height profile was taken from the red dashed line, which shows the average height of the SP-graphene flake is ~2.1 nm. Spatial Raman mapping of the D and G band intensity ratio (I_D/I_G) was collected on this SP-graphene (d) before and (e) after undergoing the two-step functionalization, and the intensity values of D and G band were calculated after fitting the peaks to Lorentzians. The step length of Raman mapping is 0.25 μm for both x and y axes, and the laser excitation wavelength was 633 nm.

and the degree of in-plane defects and functionalization in the carbon materials. In this typical set of Raman spectra, the I_D/I_G of the pristine SP-graphene was ~0.014; after the click chemistry functionalization, the I_D/I_G increased to ~0.130. The AFM image (Figure 4c) shows that the height of this graphene flake measured from a line profile is about 1.9−2.8 nm, with the average height of ~2.1 nm. It is noteworthy that the height value may be higher than that of clean and pristine bilayer graphene due to the surfactant and solvent molecules adsorbed on graphene surfaces or trapped underneath the drop-dried SP-graphene flake "coffee rings". The SP-graphene flakes on the substrates before and after the two-step functionalization were also characterized by Raman mapping (Figure 4d and e). After fitting the peaks to Lorentzians, the calculated I_D/I_G values in the Raman map of the PEG-COOH functionalized SP-graphene flake increased all throughout, demonstrating the achievement of the functionalization. The I_D/I_G spatial map indicates that the functionalization preferentially occurs at the edge and defective sites of graphene flakes but also takes place to a lesser extent on the flat graphene surface.

As mentioned above, the observation of colloidal stability after click reaction can be a metric for the grafting density since a threshold level is necessary to maintain stability after dialysis of the surfactant. We estimate this threshold by modifying the analysis developed earlier for graphene dispersion.[57] Since the surfaces of functionalized SP-graphene are charged, the mechanism of stabilization can be considered and modeled similar to surfactant-coated graphene.[58] The interaction energy, V, as a function of the separation between two functionalized graphene surfaces, r, can be described by the DLVO theory.[59] In the present model, we consider the PEG-COOH functionalized graphene sheets as double-sided, uniformly charged surfaces coated with polymer brushes, as shown in Figure 5a. As a result, the electrical potential normal to the surface, Φ, can be described by the Poisson−Boltzmann equation,[59] and the Debye−Hückel approximation is further introduced considering $e\Phi < k_BT$, where e is the elementary charge, and k_B is the Boltzmann constant. On the basis of the above approximations, the interaction energy between two parallel, functionalized graphene surfaces per unit area, V, as a function of intersheet separation, r, is given by the following equation:[58,60]

$$V(r) = 4\varepsilon_0\varepsilon_r\kappa\Phi_0^2 exp(-\kappa r) + \varepsilon\left[\left(\frac{\sigma}{r}\right)^{12} - 2\left(\frac{\sigma}{r}\right)^{6}\right] \quad (1)$$

where ε_0 is the vacuum permittivity, e_r is the relative permeativity, and Φ_0 is the electrical potential at surface. ε and σ correspond to depth and position of Lennard-Jones potential well for describing van der Waals (vdW) interactions between graphene,[57] where $\varepsilon = 0.415$ J/m^2 and $\sigma = 3.5$ nm,[57] and κ^{-1} is the Debye−Hückel screening length, which is given by the following equation:

$$\kappa^{-1} = (\varepsilon_0\varepsilon_r k_B T/e^2 n_0)^{1/2} \quad (2)$$

where n_0 is the total ion concentration of the solution. For the system considered here, n_0 should be the concentration of

dx.doi.org/10.1021/cm201131v |Chem. Mater. 2011, 23, 3362–3370

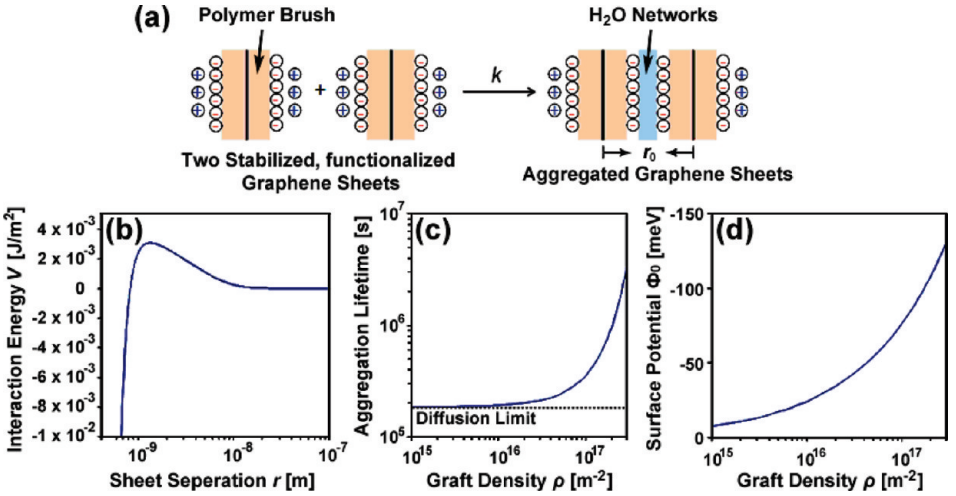

Figure 5. (a) Schematic describing the aggregation of two functionalized, monolayer graphene sheets into a bilayer complex. (b) Interaction energy between two parallel graphene sheets, V, as a function of intersheet separation, r (graft density $\rho = 1 \times 10^{17}$ m^{-2}). (c,d) Calculated aggregation lifetime (c) (the time required for the monolayer graphene sheets to be reduced by half) and the graphene surface potential (d) as a function of graft density.

hydrion only, and if the functionalized graphene sheets are 100% deprotonized, n_0 can be given by the following equation:

$$n_0 = c_g A_g \rho \tag{3}$$

where c_g is the concentration of graphene, A_g is the average area of graphene sheets, and ρ is the graft density (density of functional groups on graphene). In addition, the electrical potential at surface can be determined using Gauss' law as follows:

$$\Phi_0 = \frac{\rho e}{\varepsilon_0 \varepsilon_r \kappa} \tag{4}$$

The interactions between graphene sheets can be correlated to the kinetics of aggregation, as shown in Figure 5a. In order to quantify the kinetics of functionalized graphene sheets, several assumptions are made: (i) the aggregation process is diffusion controlled; (ii) since graphene sheets can translate and rotate freely, they are modeled as effective spheres; (iii) the lateral size of all graphene sheets is the same; (iv) the diffusivity of graphene sheets, D ($D = 1 \times 10^{-12}$ is used here),[57] is independent of its layer number, i, since the friction factor in the Stokes−Einstein relationship mainly depends on the lateral size of a graphene sheet; and (v) due to the relatively negligible thickness of the graphene sheets, the intersheet interaction potential energy is assumed to be independent of the number of layers of the two sheets. It is noteworthy that when two suspended sheets approach, all collision angles and areas are possible. Therefore, the ensemble average of all collision angles can be viewed as an effective face-to-face collision that we have considered in our analysis.

On the basis of the assumptions described above, the aggregation rate constant, k, (see Figure 5a) for all possible aggregation pairs can be expressed as follows:[57,61]

$$k = \frac{8\pi D}{\int_{r_0}^{\infty} \frac{exp(VA_C/k_BT)}{r^2}\, dr} \tag{5}$$

where A_C is the average collision area, and r_0 is the distance between two aggregated graphene sheets, as shown in Figure 5a. For the limiting case where only monolayer sheets are present initially, the aggregation process modeled above is exactly analogous to a step-polymerization reaction.[62] In that case, the concentration of monolayer graphene sheets, $N_{b1}(t)$, as a function of time, t, can be expressed analytically as follows:[62]

$$N_{b1}(t) = N_{b10}\left(\frac{1}{1 + N_{b10}kt}\right)^2 \tag{6}$$

To demonstrate this model, an arbitrary set of parameters were used ($c_g = 1 \times 10^{14}$ m^{-3}, $A_g = 1 \times 10^{-12}$ m^2, $r_0 = 6$ nm, and $A_C = 1$ nm^2), and the graft density, ρ, was set as the control parameter. The interaction energy per unit area, V, for $\rho = 10^{17}$ m^{-2} is shown in Figure 5b. The energy barrier, which increases with graft density, is responsible for repelling graphene sheets from each other. Although the aggregated state is still thermodynamically favorable, the height of the energy barrier determines the kinetic stability. The calculated lifetime for graphene dispersions (the time required for the monolayer graphene sheets to be reduced by half) and the surface electrical potential, Φ_0, as a function of graft density are shown in Figure 5c and d, respectively. Interestingly, we found that the lifetime of graphene is not greatly improved, compared to the diffusion limit, when the graft density is relatively small (<10^{15} m^{-2}) because the vdW interactions between sheets are too strong. It is noteworthy that the experimentally measured zeta-potential for our functionalized graphene dispersions is about −50 mV, which corresponds to $\Phi_0 = -60 \sim -80$ mV. As a result, the estimated graft density of our graphene dispersions should be around 10^{17} m^{-2} (one PEG-COOH group on a 10 nm^2 surface is grafted).

Moreover, to compare the reactivity of CVD-graphene with SP-graphene, the click chemistry reaction under the same conditions was also carried out on large-area single-layer CVD-graphene films transferred on SiO_2/Si chips. As shown in Figure 6a, the optical image demonstrated that the graphene film coverage on the SiO_2/Si chip is mostly continuous. Figure 6b shows the typical Raman spectra taken at the same position of the CVD-graphene film before and after the two-step functionalization. The shape of the 2D band is a single sharp Lorentzian peak instead of a sum of four peaks, and the intensity of the 2D band is higher than that of the G band. Besides, the average full-width-at-half-maximum of the 2D band is ~34 cm^{-1},

dx.doi.org/10.1021/cm201131v |Chem. Mater. 2011, 23, 3362–3370

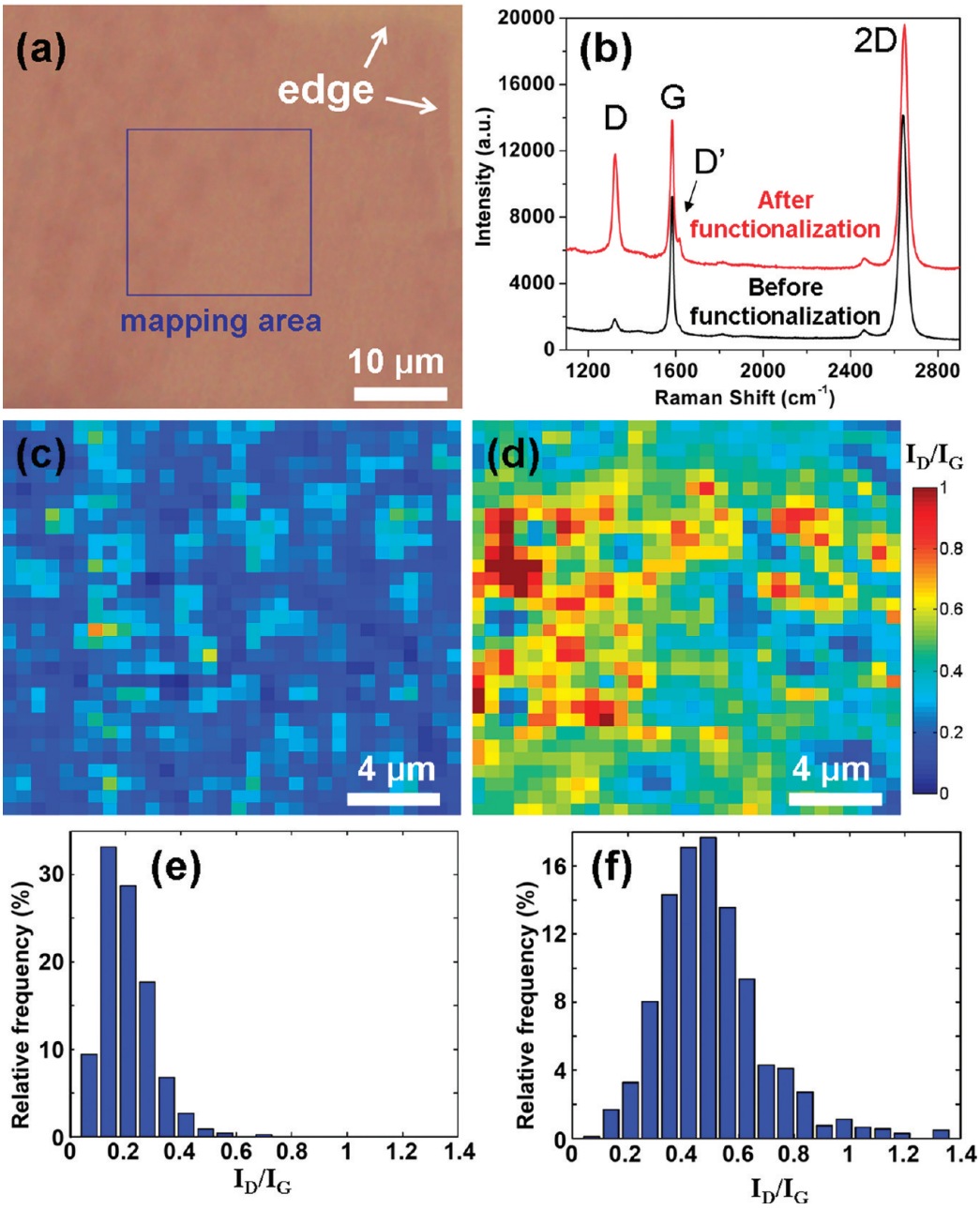

Figure 6. (a) Optical image of a large-area monolayer CVD-graphene film transferred on a SiO_2/Si chip with 300-nm-thick thermally oxidized silica. (b) Typical Raman spectra taken at the same position of this CVD-graphene film before and after the two-step functionalization. Spatial maps of I_D/I_G from Raman spectra collected at the same position of this CVD-graphene film (c) before and (d) after the two-step functionalization; the intensity values of D and G band were calculated after fitting the peaks to Lorentzians. The step length of Raman mapping was 0.6 μm for both x and y axes, and the laser excitation wavelength was 633 nm. The histograms (e and f) show the corresponding relative frequency of I_D/I_G values in the Raman spatial maps (c and d, respectively).

which is characteristic of single-layer graphene.[51] After the two-step functionalization, the G peak position of SP-graphene up-shifted from 1585 cm^{-1} to 1590 cm^{-1}, the intensity of D peak increased significantly, and an accompanied D' peak at 1622 cm^{-1} appeared, which indicates that the degree of functionalization is high. The I_D/I_G increased from ~0.10 to ~0.71, which indicates that the reactivity of CVD-graphene is higher than that of the isolated SP-graphene flake in Figure 4. Note that the higher reactivity of monolayer graphene compared to that of multilayer graphene is consistent with the previous results[22,24] and is attributed to local fluctuations in electron density that remain unscreened in monolayer graphene and increase its reactivity. Spatial Raman mapping was also collected on the CVD-graphene film, and the distribution of I_D/I_G after Lorentzian fitting are shown in Figure 6c and d. The histograms of I_D/I_G relative frequency demonstrated that the mean I_D/I_G value increased from ~0.18 to ~0.52 after the two-step functionalization. The intensity of the I_D/I_G signal at the defective sites increased much more after the PEG-COOH attachment, likely indicating that the in-plane defects or grain boundaries

dx.doi.org/10.1021/cm201131v |*Chem. Mater.* 2011, 23, 3362–3370

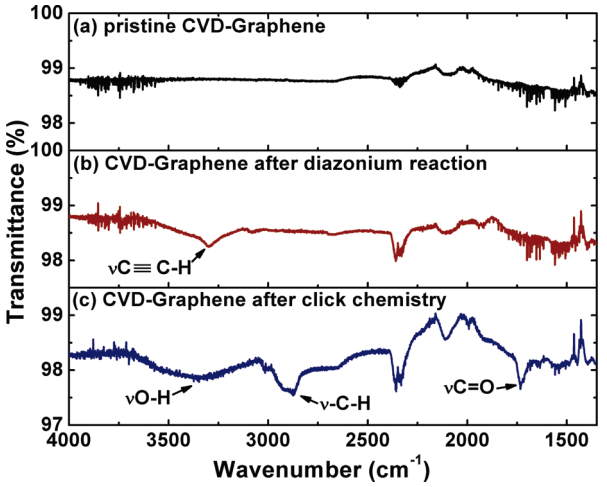

Figure 7. ATR-IR spectra of (a) pristine CVD-graphene sheets, (b) CVD-graphene after undergoing the diazonium reaction, and (c) CVD-graphene after the diazonium reaction and subsequent click chemistry reaction. All of the spectra were collected on the quartz substrates with 1 mm thickness.

of CVD-graphene sheets may enhance the click chemistry functionalization.

For the investigation of the ATR-IR spectra of pristine and functionalized CVD-graphene, we transferred the CVD-graphene sheets onto oxygen plasma cleaned quartz substrates (with 1 mm thickness) and performed the diazonium reaction and subsequent click chemistry reaction. As shown in Figure 7, the ATR-IR spectrum of pristine CVD-graphene is almost featureless and shows that the CVD-graphene sheets were free of functional groups. The CVD-graphene after the reaction with 4-Propargyloxybenzenediazonium salt shows a peak at ~3300 cm^{-1}, which can be attributed to the ≡C−H stretch. After click chemistry, the ATR-IR spectrum revealed the alkyl C−H stretching in the polyethylene glycol chains. The band at ~1730 cm^{-1} and the wide band at ~3330 cm^{-1} are, respectively, derived from the C═O stretching vibrations and O−H stretching vibrations of carboxyl groups. The peak positions are consistent with the ATR-IR data taken on the functionalized SP-graphene samples. We also conducted UV−vis absorption spectroscopy on CVD-graphene samples transferred on quartz substrates, the light transmittance of pristine and functionalized graphene over the visible frequencies range is ~98%; similar to SP-graphene solution samples, CVD-graphene shows no additional absorption peak after the functionalization.

CONCLUSIONS

In summary, we have demonstrated that 4-propargyloxybenzenediazonium functionalization and subsequent 1,3-dipolar azide−alkyne cycloaddition can be carried out on both SP-graphene and CVD-graphene sheets. Water-dispersible graphene suspended without surfactants and without oxidative treatment was successfully prepared. It is well-known that click chemistry has been broadly used for the precise covalent coupling between small molecular units at mild conditions, particularly for organic synthesis and bioconjugation. With this synthetic protocol, chemical changes can be bestowed on graphene by tailoring the functional groups on the diazonium moieties, and the subsequent reactions to attach additional moieties are allowed, thereby providing an easy and versatile route for incorporating graphene into composite materials and biosensors.

AUTHOR INFORMATION

Corresponding Author

*E-mail: strano@mit.edu.

ACKNOWLEDGMENT

We acknowledge funding from the 2009 U.S. Office of Naval Research Multi University Research Initiative (MURI) on Graphene Advanced Terahertz Engineering (GATE) at MIT, Harvard, and Boston University.

REFERENCES

(1) Geim, A. K.; Novoselov, K. S. *Nat. Mater.* **2007**, *6*, 183.
(2) Kuilla, T.; Bhadra, S.; Yao, D.; Kim, N. H.; Bose, S.; Lee, J. H. *Prog. Polym. Sci.* **2010**, *35*, 1350.
(3) Mohanty, N.; Berry, V. *Nano Lett.* **2008**, *8*, 4469.
(4) Scheuermann, G. M.; Rumi, L.; Steurer, P.; Bannwarth, W.; Mulhaupt, R. *J. Am. Chem. Soc.* **2009**, *131*, 8262.
(5) Frazier, R. M.; Daly, D. T.; Swatloski, R. P.; Hathcock, K. W.; South, C. R. *Recent Pat. Nanotechnol.* **2009**, *3*, 164.
(6) Ruoff, R. *Nat. Nanotechnol.* **2008**, *3*, 10.
(7) Hummers, W. S.; Offeman, R. E. *J. Am. Chem. Soc.* **1958**, *80*, 1339.
(8) Schniepp, H. C.; Li, J. L.; McAllister, M. J.; Sai, H.; Herrera-Alonso, M.; Adamson, D. H.; Prud'homme, R. K.; Car, R.; Saville, D. A.; Aksay, I. A. *J. Phys. Chem. B* **2006**, *110*, 8535.
(9) Dikin, D. A.; Stankovich, S.; Zimney, E. J.; Piner, R. D.; Dommett, G. H. B.; Evmenenko, G.; Nguyen, S. T.; Ruoff, R. S. *Nature* **2007**, *448*, 457.
(10) Kosynkin, D. V.; Higginbotham, A. L.; Sinitskii, A.; Lomeda, J. R.; Dimiev, A.; Price, B. K.; Tour, J. M. *Nature* **2009**, *458*, 872.
(11) Dreyer, D. R.; Park, S.; Bielawski, C. W.; Ruoff, R. S. *Chem. Soc. Rev.* **2010**, *39*, 228.
(12) Szabó, T.; Berkesi, O.; Forgó, P.; Josepovits, K.; Sanakis, Y.; Petridis, D.; Dékány, I. *Chem. Mater.* **2006**, *18*, 2740.
(13) Mkhoyan, K. A.; Contryman, A. W.; Silcox, J.; Stewart, D. A.; Eda, G.; Mattevi, C.; Miller, S.; Chhowalla, M. *Nano Lett.* **2009**, *9*, 1058.
(14) Park, S.; Ruoff, R. S. *Nat. Nanotechnol.* **2009**, *4*, 217.
(15) Konatham, D.; Striolo, A. *Nano Lett.* **2008**, *8*, 4630.
(16) Si, Y.; Samulski, E. T. *Nano Lett.* **2008**, *8*, 1679.
(17) Fang, M.; Wang, K. G.; Lu, H. B.; Yang, Y. L.; Nutt, S. *J. Mater. Chem.* **2009**, *19*, 7098.
(18) Satti, A.; Larpent, P.; Gun'ko, Y. *Carbon* **2010**, *48*, 3376.
(19) Choi, E. K.; Jeon, I. Y.; Oh, S. J.; Baek, J. B. *J. Mater. Chem.* **2010**, *20*, 10936.
(20) Farmer, D. B.; Golizadeh-Mojarad, R.; Perebeinos, V.; Lin, Y. M.; Tulevski, G. S.; Tsang, J. C.; Avouris, P. *Nano Lett.* **2009**, *9*, 388.
(21) Farmer, D. B.; Lin, Y. M.; Afzali-Ardakani, A.; Avouris, P. *Appl. Phys. Lett.* **2009**, *94*, 213106.
(22) Koehler, F. M.; Jacobsen, A.; Ensslin, K.; Stampfer, C.; Stark, W. J. *Small* **2010**, *6*, 1125.
(23) Lim, H.; Lee, J. S.; Shin, H. J.; Shin, H. S.; Choi, H. C. *Langmuir* **2010**, *26*, 12278.
(24) Sharma, R.; Baik, J. H.; Perera, C. J.; Strano, M. S. *Nano Lett.* **2010**, *10*, 398.
(25) Bekyarova, E.; Itkis, M. E.; Ramesh, P.; Berger, C.; Sprinkle, M.; de Heer, W. A.; Haddon, R. C. *J. Am. Chem. Soc.* **2009**, *131*, 1336.
(26) Hossain, M. Z.; Walsh, M. A.; Hersam, M. C. *J. Am. Chem. Soc.* **2010**, *132*, 15399.
(27) Sinitskii, A.; Dimiev, A.; Corley, D. A.; Fursina, A. A.; Kosynkin, D. V.; Tour, J. M. *ACS Nano* **2010**, *4*, 1949.

(28) Lomeda, J. R.; Doyle, C. D.; Kosynkin, D. V.; Hwang, W. F.; Tour, J. M. *J. Am. Chem. Soc.* **2008**, *130*, 16201.
(29) Englert, J. M.; Dotzer, C.; Yang, G.; Schmid, M.; Papp, C.; Gottfried, J. M.; Steinück, H.-P.; Spiecker, E.; Hauke, F.; Hirsch, A. *Nat. Chem.* **2011**, *3*, 279.
(30) Fan, X. Y.; Nouchi, R.; Yin, L. C.; Tanigaki, K. *Nanotechnology* **2010**, 21.
(31) Niyogi, S.; Bekyarova, E.; Itkis, M. E.; Zhang, H.; Shepperd, K.; Hicks, J.; Sprinkle, M.; Berger, C.; Lau, C. N.; deHeer, W. A.; Conrad, E. H.; Haddon, R. C. *Nano Lett.* **2010**, *10*, 4061.
(32) Fang, M.; Wang, K. G.; Lu, H. B.; Yang, Y. L.; Nutt, S. *J. Mater. Chem.* **2010**, *20*, 1982.
(33) Bahr, J. L.; Yang, J. P.; Kosynkin, D. V.; Bronikowski, M. J.; Smalley, R. E.; Tour, J. M. *J. Am. Chem. Soc.* **2001**, *123*, 6536.
(34) Niyogi, S.; Hamon, M. A.; Hu, H.; Zhao, B.; Bhowmik, P.; Sen, R.; Itkis, M. E.; Haddon, R. C. *Acc. Chem. Res.* **2002**, *35*, 1105.
(35) Jiang, D. E.; Sumpter, B. G.; Dai, S. *J. Chem. Phys.* **2007**, *126*, 134701.
(36) Sun, Z. Z.; Kohama, S.; Zhang, Z. X.; Lomeda, J. R.; Tour, J. M. *Nano Res.* **2010**, *3*, 117.
(37) Rodionov, V. O.; Presolski, S. I.; Diaz, D. D.; Fokin, V. V.; Finn, M. G. *J. Am. Chem. Soc.* **2007**, *129*, 12705.
(38) Hein, J. E.; Fokin, V. V. *Chem. Soc. Rev.* **2010**, *39*, 1302.
(39) Moses, J. E.; Moorhouse, A. D. *Chem. Soc. Rev.* **2007**, *36*, 1249.
(40) Devadoss, A.; Chidsey, C. E. D. *J. Am. Chem. Soc.* **2007**, *129*, 5370.
(41) Kiick, K. L.; Saxon, E.; Tirrell, D. A.; Bertozzi, C. R. *Proc. Natl. Acad. Sci. U.S.A.* **2002**, *99*, 19.
(42) Hong, V.; Presolski, S. I.; Ma, C.; Finn, M. G. *Angew. Chem., Int. Ed.* **2009**, *48*, 9879.
(43) Boisselier, E.; Salmon, L.; Ruiz, J.; Astruc, D. *Chem. Commun.* **2008**, 5788.
(44) Kinge, S.; Gang, T. A.; Naber, W. J. M.; van der Wiel, W. G.; Reinhoudt, D. N. *Langmuir* **2011**, *27*, 570.
(45) Li, H. M.; Cheng, F. O.; Duft, A. M.; Adronov, A. *J. Am. Chem. Soc.* **2005**, *127*, 14518.
(46) Salvio, R.; Krabbenborg, S.; Naber, W. J. M.; Velders, A. H.; Reinhoudt, D. N.; van der Wiel, W. G. *Chem.—Eur. J.* **2009**, *15*, 8235.
(47) Sun, S. T.; Cao, Y. W.; Feng, J. C.; Wu, P. Y. *J. Mater. Chem.* **2010**, *20*, 5605.
(48) Shih, C.-J.; Vijayaraghavan, A.; Krishnan, R.; Sharma, R.; Han, J.-H.; Ham, M.-H.; Jin, Z.; Lin, S.; Paulus, G. L. C.; Reuel, N. F.; Wang, Q. H.; Blankschtein, D.; Strano, M. S. *Nat. Nanotechnol.* **2011**, doi:10.1038/nnano.2011.94.
(49) Jin, Z.; Yao, J.; Kittrell, C.; Tour, J. M. *ACS Nano* **2011**, *5*, 4114.
(50) Deegan, R. D.; Bakajin, O.; Dupont, T. F.; Huber, G.; Nagel, S. R.; Witten, T. A. *Nature* **1997**, *389*, 827.
(51) Li, X. S.; Cai, W. W.; An, J. H.; Kim, S.; Nah, J.; Yang, D. X.; Piner, R.; Velamakanni, A.; Jung, I.; Tutuc, E.; Banerjee, S. K.; Colombo, L.; Ruoff, R. S. *Science* **2009**, *324*, 1312.
(52) Seyedi, S. M.; Jafari, Z.; Attaran, N.; Sadeghian, H.; Saberi, M. R.; Riazi, M. M. *Bioorg. Med. Chem.* **2009**, *17*, 1614.
(53) Wong, L. S.; Janusz, S. J.; Sun, S.; Leggett, G. J.; Micklefield, J. *Chem.—Eur. J.* **2010**, *16*, 12234.
(54) Ferrari, A. C.; Meyer, J. C.; Scardaci, V.; Casiraghi, C.; Lazzeri, M.; Mauri, F.; Piscanec, S.; Jiang, D.; Novoselov, K. S.; Roth, S.; Geim, A. K. *Phys. Rev. Lett.* **2006**, *97*, 187401.
(55) De Marco, P.; Nardone, M.; Vitto, A. D.; Alessandri, M.; Santucci, S.; Ottaviano, L. *Nanotechnology* **2010**, *21*, 255703.
(56) Graf, D; M., F.; E., K.; S., C.; J., A.; H., C.; W., L. *Nano Lett.* **2007**, *7*, 238.
(57) Shih, C. J.; Lin, S. C.; Strano, M. S.; Blankschtein, D. *J. Am. Chem. Soc.* **2010**, *132*, 14638.
(58) Lotya, M. H., Y.; King, P. J.; Smith, R. J.; Nicolosi, V.; Karlsson, L. S.; Blighe, F. M.; De, S.; Wang, Z. M.; McGovern, I. T.; Duesberg, G. S.; Coleman, J. N. *J. Am. Chem. Soc.* **2009**, *131*, 3611.
(59) Israelachvili, J. N. *Philos. Mag. A* **1981**, *43*, 753.
(60) Israelachvili, J. N.; Tandon, R. K.; White, L. R. *J. Colloid Interface Sci.* **1980**, *78*, 430.
(61) Fuchs, N. *Z. Phys. Chem. Abt. A* **1934**, *171*, 199.
(62) Dotson, N. A. *Polymerization Process Modeling*; VCH: New York, 1996.